Pergamon

Corrosion Science, Vol. 40, No. 2/3, pp. 431–438, 1998

Printed in Great Britain.
0010-938X/98 $19.00+0.00

PII: S0010-938X(97)00149-2

CHEMICAL ANALYSIS OF PASSIVE FILMS ON TYPE AISI 304 STAINLESS STEEL USING SOFT X-RAY ABSORPTION SPECTROSCOPY

J. M. BASTIDAS, M. F. LÓPEZ, A. GUTIÉRREZ and C. L. TORRES

Centro Nacional de Investigaciones Metalúrgicas, CSIC, Avda. Gregorio del Amo 8, 28040 Madrid, Spain

Abstract—X-ray absorption spectroscopy has been employed to investigate the differences between passive films on type AISI 304 stainless steel produced by anodic polarization at two scan rates and four potential values. Cr $L_{III,II}$ spectra show that in all cases a Cr_2O_3 film is formed at the surface. Fe and Ni signals have a mainly metallic lineshape with a possible small contribution from hydroxides, which is maximum for the polarized sample at the slowest scan rate and the maximum potential. Also for this sample a decrease in the Mn signal indicates Mn dissolution. © 1998 Elsevier Science Ltd. All rights reserved

Keywords: A. stainless steel, B. polarization, C. pitting corrosion, soft x-ray absorption spectroscopy (XAS).

INTRODUCTION

The solid state properties of passive films formed on stainless steel (ss) have been widely studied using x-ray photoelectron spectroscopy (XPS) and Auger electron spectroscopy (AES) techniques.[1–5] A Cr-rich film on the surface, with some amount of hydroxides and water containing compounds, concentrates at the outermost layers. This film is responsible for maintaining passivity in these materials.[5] The Cr enriched phase in the passive film, which is formed on AISI 304 ss when immersed in sulphuric acid, depends on the time and potential of passivation and on the existence of chloride ions in the electrolyte.[4]

X-ray absorption spectroscopy (XAS) is a widely used technique to investigate chemical and electronic properties of materials.[6–8] Since the absorption process involves two different electronic levels (one core level and one empty level above the Fermi energy), this technique is extremely sensitive to the chemical state and symmetry properties of the emitting atom.[9] For a number of transition metals, the $L_{III,II}$ edges have been extensively studied both from fundamental and technological points of view,[10,11] but only a few works have been devoted to studying ss material.[12,13]

The aim of this work is to study by XAS the structure and the chemical composition of the passive films formed on a type AISI 304 ss surface, using two polarization scan rates and two polarization regions.

Manuscript received 14 November 1996; in amended form 18 September 1997

METHODS AND MATERIALS

The samples under study, of type AISI 304 austenitic ss, had the following chemical composition (wt%) 19.7 Cr, 9.4 Ni, 0.036 C, 0.003 S, 1.70 Mn, 0.28 Si, 0.022 P, 0.319 Mo with the balance in Fe. Specimens of 1 cm × 1 cm were cut from a 4 mm thick plate, embedded in cold epoxy resin and mechanically polished with successive SiC of 120, 400 and 600 grain size, followed with alumina and finally, diamond paste of 1 μm grain size.

500 ml of a 5% NaCl aqueous solution (pH ~ 8) was used as electrolyte, prepared from reagent grade NaCl and distilled water. The electrochemical cell used was similar to the ASTM G-5 standard. In order to simulate service conditions more closely, no purge gas was employed. All experiments were carried out at room temperature.

Anodic polarization curves were performed after 30 min exposure to the test solution, starting at the open-circuit potential. An EG&G PARC 273A potentiostat was used in the three-electrode configuration. A saturated calomel electrode (SCE) and a platinum spiral wire of large area were used as reference and counter electrodes, respectively. Two sweep rates were used: 0.16 and 5.0 mV s^{-1}.

After polarization tests, the samples were extracted from the electrochemical cell, rinsed in distilled water, dried with hot air, removed from the epoxy resin and stored in a desiccator until they were placed in the ultrahigh vacuum (UHV) chamber for the XAS measurements.

XAS experiments were conducted to determine the chemical composition of the polarized AISI 304 ss surfaces at two regions: (i) at the passive region, which corresponds to samples labelled 'A' and 'C', and (ii) at the pitting region, which corresponds to samples labelled 'B' and 'D'. Additionally, and for comparative purposes, three types of samples were used: (a) an unpolarized AISI 304 ss, with identical surface preparation as described above for polarized samples; (b) Fe, Cr and Ni pure metal samples in the form of polycrystalline material. In order to remove the native oxide layer, these samples were scraped inside the UHV chamber. The oxygen K-threshold absorption signal was negligible; and (c) FeO, oxidized Cr and NiO samples. The FeO sample was also scraped inside the UHV chamber in order to remove other oxides from the surface. The oxidized Cr was obtained by air exposure of Cr metal, i.e., a native oxide layer was generated on the Cr metal surface.

The XAS measurements were performed at the SX700/II soft x-ray monochromator operated by the Freie Universität Berlin at the Berliner Elektronenspeicherring für Synchrotronstrahlung (BESSY). XAS spectra were obtained at the L_{III} and L_{II} absorption thresholds by recording the total yield of secondary electrons from the sample surfaces, i.e., in total electron yield mode (TEY). The probe depth of XAS in TEY mode is ~ 100 Å.[14] The base pressure in the UHV-chamber during the measurements was better than 2×10^{-10} Torr.

RESULTS AND DISCUSSION

Figure 1 shows two typical anodic polarization curves for an AISI 304 ss immmersed in a 5% NaCl aqueous solution at two sweep rates, 0.16 and 5.0 mV s^{-1}. At relatively low anodic polarization, the current density increases with increasing anodic potential. In this region, the anodic current density only corresponds to the dissolution of the film covering AISI 304 ss. After that, the passive state is achieved. After this passivity plateau, there is an abrupt enhancement of the anodic current density as a function of time.[15] The onset of this enhancement defines the so-called nucleation pit potential (E_{np}).[16] Figure 1 also shows

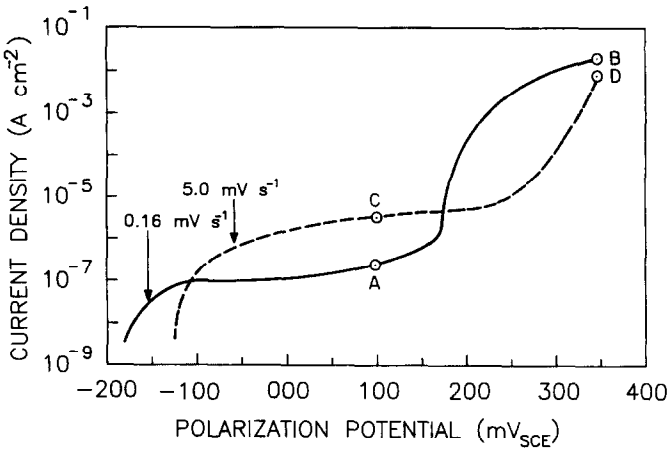

Fig. 1. Typical anodic polarization treatments of AISI 304 stainless steel at scan rates of 0.16 and 5.0 mV s^{-1}. The electrolyte used was a 5% NaCl.

that as the polarization scan rate increases from 0.16 to 5.0 mV s^{-1} the E_{np} shifts to more anodic values, from +170 mV$_{SCE}$ to +270 mV$_{SCE}$.

Figure 2 depicts the iron L_{III} and L_{II} x-ray absorption threshold spectra for the four polarized and unpolarized AISI 304 ss samples, as well as for Fe metal and FeO. In general, the shape of all AISI 304 ss spectra is similar to the Fe metal sample, though some differences indicating the presence of additional species can be observed. On unpolarized ss and samples A, B, C and D, the main peak at the L_{III} threshold is narrower than in the case of the Fe metal sample. Furthermore, a small shoulder, located at $h\nu \sim 708.5$ eV, can be observed. This structure is indicated by the arrow. The spectrum of FeO (Fig. 2 bottom) is also different to the AISI 304 ss spectra, showing a broader L_{III} peak and an additional structure at the L_{II} edge, located at ~721 eV. This excludes the presence of Fe^{2+} oxides in the AISI 304 ss spectra. Therefore, the spectral differences between the AISI 304 ss and Fe metal cannot be attributed to FeO, either Fe_2O_3 or Fe_3O_4, because the spectral shape of AISI 304 ss is different to the two oxides.[17] Since the samples have interacted with an electrolyte, a possibility would be the presence of a small amount of hydroxide compounds or hydrated molecules, with the metallic contribution being predominant. These compounds would induce a decrease in the crystal field around the Fe^{3+} ion, in contrast with the oxide which can lead to the observed spectral features.[18]

On the spectrum of sample B (Fig. 2), the differences with the Fe metal spectrum become more evident. The shoulder located at 708.5 eV is more intense and the L_{III} peak is narrower than for the other AISI 304 ss samples, indicating a higher ammount of hydroxides in this sample. Also at the L_{II} threshold, some differences are visible between, on the one hand, sample B and the unpolarized sample and, on the other hand, samples A, C and D AISI 304 ss; the former exhibiting a small shoulder located at ~723 eV. This behaviour may be attributed to the different polarization applied which produces a different amount of hydroxides. Whereas samples A and C were obtained at the passive region and, on sample D, very few pits were visually observed at 40 × in an optical microscope, sample B presented a higher number of pits, meaning that in this case the substrate beneath the passive film is more easily attacked.

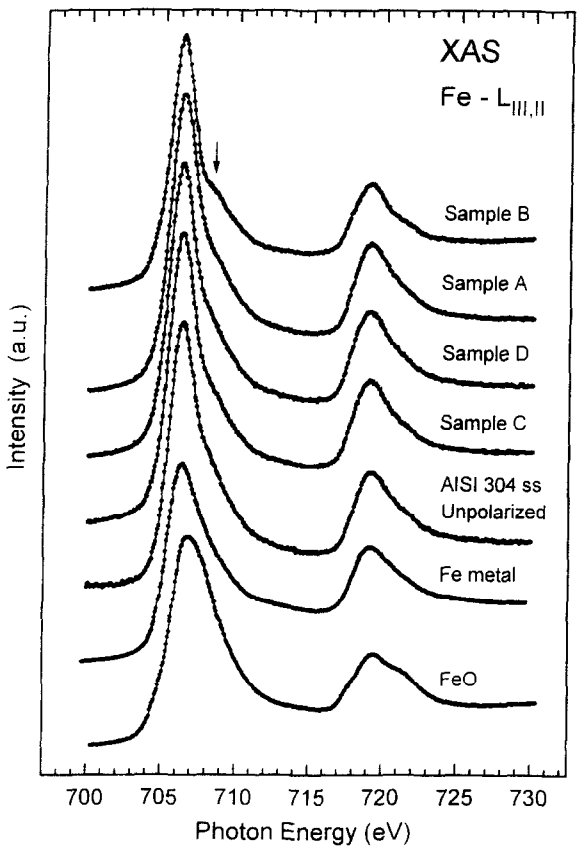

Fig. 2. Iron L_{III} and L_{II} x-ray absorption spectra for unpolarized, polarized A, B, C and D (see Fig. 1) AISI 304 stainless steel (ss), Fe metal and FeO samples.

Figure 3 displays the chromium L_{III} and L_{II} x-ray absorption threshold spectra for the four polarized and unpolarized AISI 304 ss samples as well as for oxidized Cr and Cr metal samples. In all AISI 304 ss samples, the presence of Cr_2O_3 can be clearly observed.[17] The oxidized Cr spectrum consists of a mixture of Cr_2O_3 and metallic chromium. In order to compare the passive film thickness of the different samples studied, a simple quantitative analysis based on the intensity ratio between the two main peaks at the L_{III} edge, at 575.2 eV and 567.7 eV respectively, was performed. The higher the relative intensity of the first peak, the higher the metallic chromium component. This analysis gives a value of 1.66 for sample B and 1.50 ± 0.01 for all the other samples, indicating a higher metallic component in the case of sample B. Nevertheless, the metallic contribution for all AISI 304 ss samples is very small since the spectra are very similar to Cr_2O_3.

Figure 4 presents the nickel L_{III} and L_{II} x-ray absorption threshold spectra for the four polarized and unpolarized AISI 304 ss, Ni metal and NiO samples. In general, the AISI 304 ss spectra are similar to that of Ni metal. The shake-up satellite peak located at ~ 859 eV is typical of metallic Ni and cannot be observed in the NiO sample. In the spectrum of sample B, the peak corresponding to the L_{II} edge has a slightly different shape to the other AISI 304 ss samples. This spectral shape is similar to the double structure observed at the

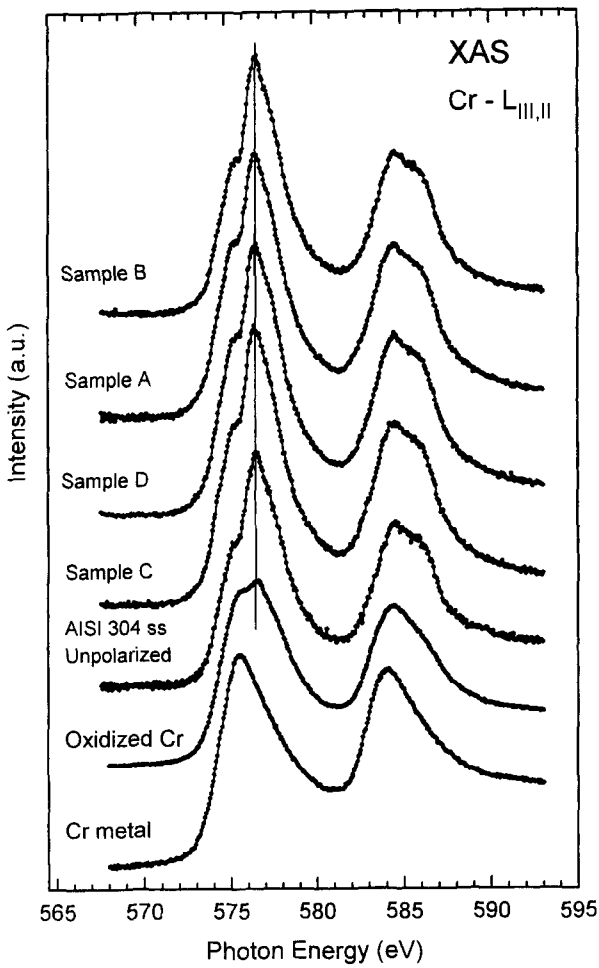

Fig. 3. Chromium L_{III} and L_{II} x-ray absorption spectra for unpolarized, polarized A, B, C and D (see Fig. 1) 304 stainless steel (ss), Oxidized Cr and Cr metal samples.

L_{II} edge of the NiO sample. As was stated above for Fig. 2, as the number of pits increases, the base metal is more readily attacked. It is possible to make a quantitative analysis based on the XAS spectra by comparing the peak to pre-edge intensity at the L_{III} threshold. For this purpose, all the AISI 304 ss spectra in Fig. 4 were normalized to the intensity at the L_{III} pre-edge in such a way that the intensity of the L_{III} main peak is a direct indication of the relative amount of Ni in each sample. Whereas the Ni content of the four polarized AISI 304 ss samples is approximately the same, the unpolarized AISI 304 ss sample shows a much higher Ni intensity (almost twice as much). This result suggests that the polarization treatment induces Ni depletion at the AISI 304 ss surface. The Fe/Cr and Ni/Cr signals in the 'scraped' and passivated AISI 304 ss spectra support the hypothesis that a small amount of substrate is being sampled in the iron and nickel passive film spectra. Olefjord and Wegrelius have shown that nickel is not present in the oxide film, while the film is depleted in iron compared to the substrate.[19] Thus, all of the nickel signal arises from the substrate, while most of the iron signal arises from the substrate.

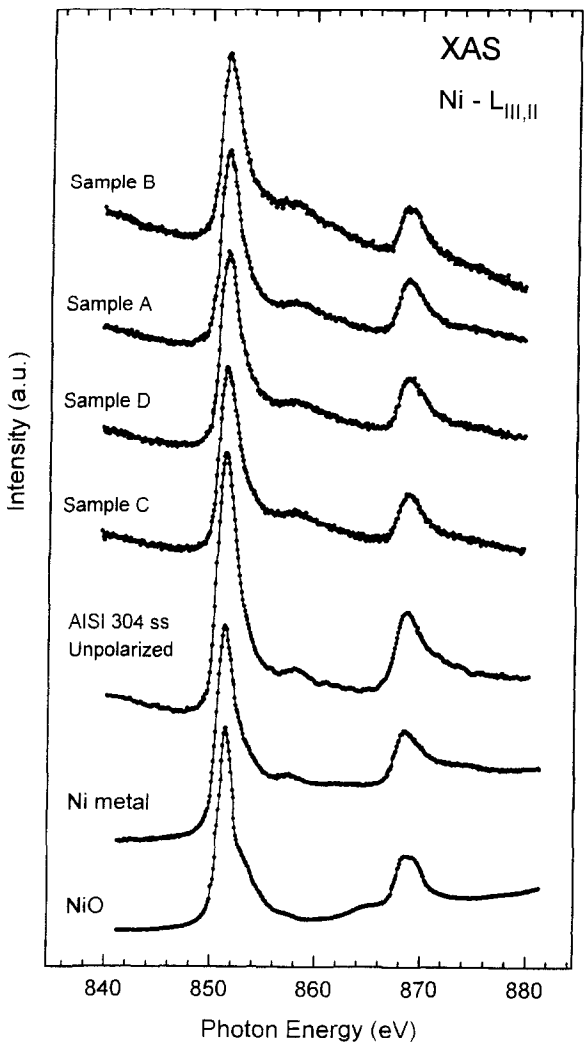

Fig. 4. Nickel L_{III} and L_{II} x-ray absorption spectra for unpolarized, polarized A, B, C and D (see Fig. 1) 304 stainless steel (ss), Ni metal and NiO samples.

Figure 5 includes manganese L_{III} and L_{II} spectra for unpolarized and polarized AISI 304 ss samples. In general, the shape of the spectra is similar in all cases under study. Figure 5 was obtained in a similar way to Fig. 4, i.e. after a normalization procedure. The intensity of the peak for sample B is smaller ($\sim 2/3$) than for the other samples. This behaviour suggests Mn dissolution at the pitting areas.

CONCLUSIONS

Electrochemical results indicate that as the polarization scan rate increases from 0.16 to 5.0 mV s^{-1}, the nucleation pit potential takes more noble values: from $+170\,mV_{SCE}$ to

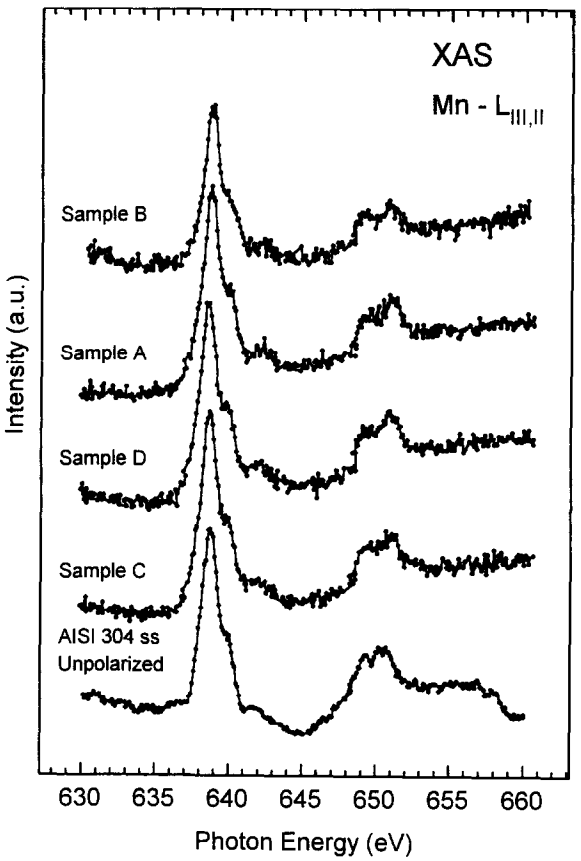

Fig. 5. Manganese L_{III} and L_{II} x-ray absorption spectra for unpolarized and polarized A, B, C and D (see Fig. 1) 304 stainless steel (ss) samples.

$+270\,mV_{SCE}$ respectively. Also the passivity plateau is expanded: 200 mV for $0.16\,mV\,s^{-1}$ and 250 mV for $5.0\,mV\,s^{-1}$.

XAS spectra of all AISI 304 ss samples at the Fe and Ni $L_{II,III}$ absorption thresholds have a similar line shape to metallic Fe and Ni, suggesting that iron and nickel are not present in the oxide film. The anodic polarization treatment causes Ni depletion at the surface as shown by the fact that the intensity of the Ni L_{III} peak is lower for all the polarized samples than for the unpolarized sample. Some differences are observed at the Fe $L_{III,II}$ absorption edge between the AISI 304 ss samples and the Fe metal sample which may be related to the formation of a small amount of hydroxide compounds. These differences are more evident for the sample polarized at the lowest scan rate ($0.16\,mV\,s^{-1}$) and at the highest potential ($+350\,mV_{SCE}$) where more pits can be visually observed. Also, for this sample, a slightly oxidized Ni component can be observed and a decrease in the Mn signal associated to Mn dissolution.

Acknowledgements—This work has been supported by the Spanish Interministerial Science and Technology Commission (CICYT) under Project No. MAT95-2004-E and by the BESSY-EU Project No. CHGE-CT93-0027. The authors wish to thank M. Domke and the BESSY staff for their help during the XAS experiments.

REFERENCES

1. Lorang, G., Da Cunha Belo, M., Simoes, A.M.P. and Ferreira, M.G.S. *J. Electrochem. Soc.*, 1994, **141,** 3347.
2. Asami, K., Hashimoto, K. and Shimodaira, S. *Corros. Sci.*, 1978, **18,** 151.
3. Mathieu, H.J. and Landolt, D. *Corros. Sci.*, 1986, **26,** 547.
4. Brooks, A.R., Clayton, C.R., Doss, K. and Lu, Y.C. *J. Electrochem. Soc.*, 1986, **133,** 2459.
5. Kirchheim, R., Heine, B., Fischmeister, H., Hofmann, S., Knote, H. and Stolz, U. *Corros. Sci.*, 1989, **29,** 899.
6. Gutiérrez, A., Díaz, J. and López, M.F. *Appl. Phys. A Mater.*, 1995, **61,** 111.
7. Pellegrin, E., Nücker, N., Fink, J., Molodtsov, S.L., Gutiérrez, A., Navas, E., Strebel, O., Hu, Z., Domke, M., Kaindl, G., Uchida, S., Nakamura, Y., Markl, J., Klauda, M., Saemann-Ischenko, G., Krol, A., Peng, J.L., Li, Z.Y. and Greene, R.L. *Phys. Rev. B*, 1993, **47,** 3354.
8. Abbate, M., de Groot, F.M.F., Fuggle, J.C., Fujimori, A., Strebel, O., Lopez, F., Domke, M., Kaindl, G., Sawatzky, G.A., Takano, M., Takeda, Y., Eisaki, H. and Uchida, S. *Phys. Rev. B*, 1992, **46,** 4511.
9. de Groot, F.M.F. *J. Electron Spectrosc.*, 1994, **67,** 529.
10. Crocombette, J.P., Pollak, M., Jollet, F., Thromat, N. and Gautier-Soyer, M. *Phys. Rev. B*, 1995, **52,** 3143.
11. de Groot, F.M.F., Hu, Z.W., López, M.F., Kaindl, G., Guillot, F. and Tronc, M. *J. Chem. Phys.*, 1994, **101,** 6570.
12. Davenport, A.J., Sansone, M., Bardwell, J.A., Aldykiewicz, A.J. Jr., Taube, M. and Vitus, C.M. *J. Electrochem. Soc.*, 1994, **141,** L6.
13. Barret, N.T., Gibson, P.N., Greaves, G.N., Roberts, K.J. and Sacchi, M. *Physica B*, 1989, **158,** 690.
14. Abbate, M., Goedkoop, J.B., de Groot, F.M.F., Grioni, M., Fuggle, J.C., Hofmann, S., Petersen, H. and Sacchi, M. *Surf. Interface Anal.*, 1992, **18,** 65.
15. Scully, J.C. *Corros. Australas.*, 1982, **7,** 4.
16. Szklarska-Smialowska, Z. and Janik-Czachor, M. *Corros. Sci.*, 1971, **11,** 901.
17. Soriano, L., Abbate, M., de Groot, F.M.F., Alders, D., Fuggle, J.C., Hofmann, S., Petersen, H. and Braun, W. *Surf. Interface Anal.*, 1993, **20,** 21.
18. de Groot, F.M.F., Fuggle, J.C., Thole, B.T. and Sawatzky, G.A. *Phys. Rev. B*, 1990, **42,** 5459.
19. Olefjord, I. and Wegrelius, L. *Corros. Sci.*, 1990, **31,** 89.